4D Non Local regularization of 3D seismic data using block adaptive POCS

Satyakee Sen, James Sheng, Zhaojun Liu and Bin Wang, TGS

Summary

We describe a new transform domain-based regularization scheme where the sparsity constraint is applied nonlocally to a group of windows that have similar signal content. Unlike existing regularization methods that work on individual overlapping windows, one at a time, our method searches the dataset for windows with similar signal content to the current window of interest. All such similar windows are then put together to form an adaptive window block (AWB), adaptive in the sense that all windows within the block have similar signal content. The uplift of using an AWB is the increased sparsity and low rank structure of the true signal within the block when compared to a single window. A modified projection onto convex sets (POCS) type scheme is then performed on the AWB to regularize the data. Since this modified POCS works on adapted blocks of windows we call it block adaptive POCS (BAPOCS). Using 3D supershot gathers from both a WAZ and NAZ survey from the Gulf of Mexico (GOM) we show the significant improvement that can be achieved in the RTM image by using our BAPOCS method.

Introduction

Seismic data is inherently redundant and repetitive. Similar dips and similar structures appear throughout a dataset due to the consistency of the subsurface geology that we are trying to image. However almost all existing seismic data regularization methods like POCS (Abma et al., 2006), anti-leakage fourier transform (ALFT, Xu et al., 2005), sparse tau-*p* (Wang et al., 2014) do not explicitly exploit this natural redundancy and repetitiveness, instead all these methods work on individual windows, one at a time (windows can be 3D, 4D or 5D depending on the dimensions of the data). Recently developed nonlocal (NL) methods in the field of image processing have shown that exploiting redundancy in images, by allowing individual windows to communicate and share information can vastly improve applications like image denoising and reconstruction. In fact NL methods are considered to be the state of the art (Buades et al., 2011) when it comes to these applications in image processing. Examples of such nonlocal methods include nonlocal means (Buades et al., 2005), block matching 3D, BM3D (Dabov et al., 2007), to name a few.

In this paper we present a method (BAPOCS) where NL-processing techniques using AWBs are included within a well-studied existing seismic data regularization scheme (POCS) using the BM3D framework developed by Dabov et al. We demonstrate with real data examples the superior uplift that can be achieved using our BAPOCS method. Although we focus on including NL techniques into the POCS scheme, it is relatively straightforward to incorporate NL techniques into almost any other transform domain based regularization scheme, such as ALFT.

Theory

The underlying assumption in a transform domain (e.g., Fourier domain) regularization method is that the true signal is inherently low dimensional and compressible in the transform domain. Thus it can be effectively separated from the regularization noise, which is random and devoid of structure, by an L1 inversion using thresholding and shrinkage of transform domain coefficients (e.g., POCS, ALFT, and Sparse Tau-P). However whether a typical seismic dataset with irregular trace distribution, missing traces, holes etc. is truly compressive or not in the transform domain is debatable. A logical approach then would be to try and use schemes that can explicitly enhance the sparsity of the seismic data in the transform domain. BM3D is a well-known NL technique that attempts to do this for natural images to improve thresholding and shrinkage-based denoising. In this abstract we describe how BM3D's NL principles are modified and adapted for 3D seismic data regularization within a POCS scheme. The main steps for a typical 3D supershot receiver patch regularization scheme using BAPOCS are described below. The method's applicability to other types of datasets (example offset cubes) remains unchanged.

STEP 1: Forming the adaptive window block (AWB)

The key step in our method is the creation of the AWB which allows NL processing techniques to be introduced into the regularization problem. For the current 3D window of interest (W_{ref}) in a supershot gather, a search is performed within a user-determined radius around W_{ref} (within the same supershot and across neighboring supershots) to find other windows of similar signal content. The similarity is defined based on the normalized Euclidean distance (*d*) between the window of interest (W_{ref}) and other windows (W_{other}), computed on a low-pass filtered version of the windows, as:

$$d\left(W_{ref}, W_{other}\right) = \left\|W_{ref} - W_{other}\right\|_2^2 / \left\|W_{ref}\right\|_2^2$$

Computing the similarity on a low-pass filtered version ensures that problems due to aliasing are not encountered. If the computed normalized distance for the window, W_{other}, is smaller than a user-defined threshold, then W_{other} is included as part of the window block. Once such windows are found, they are put together one behind the other (in decreasing order of similarity) to create the AWB. Figure 1 shows the process for 2D windows. In general for computation efficiency we limit the number of windows included in the AWB to be between 8-10. Notice that unlike the sparse tau-*p* based supershot regularization proposed by Wang et al, 2014, our method can naturally incorporate crossshot information.

For a 3D supershot, Step 1 turns a 3D window into a 4D window block thus increasing the dimensionality of the data. Note that by construction within the AWB the signal characteristics are highly similar along the newly introduced 4th dimension (window-index dimension in Figure 1), thus the true signal has a low rank structure and much higher degree of compressibility in the higher dimensional Fourier transformed AWB space (4D space) as compared to the corresponding lower dimensional Fourier transformed single individual window (3D space). In essence, the AWB construction ensures, that irrespective of the nature of the dataset, transform domain sparsity is enhanced to facilitate better thresholding and signal recovery.

STEP 2: Block Adaptive POCS (BAPOCS) Iteration

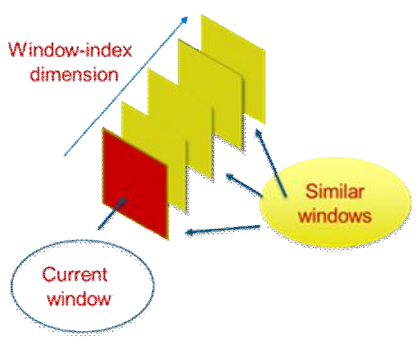

Figure 1: 3D Adaptive window block construction, 2D windows similar (yellow) to the current window (red) are stacked together to form a 3D window block, additional dimension is the window-index.

Similar to a regular POCS, the regularization stage begins by performing an FFT along all axes of the AWB. Unlike 3D POCS which requires a 3D-FFT for the window, here a 4D FFT is performed on the window block. Since several different windows are simultaneously transformed to the Fourier domain as a block, the concept of Collaborative Filtering (Xu, 2009) comes into play. Each window within the block collaborates with each other to improve the signal identification and thresholding task at each POCS iteration. For a window block the number of significant coefficients needed to represent the data is much smaller than if each window was individually transformed to the Fourier domain (due to the low frequency dominance along the added window dimension). Care is taken during the thresholding process that the DC component and the low frequencies around the DC component are extracted unchanged along the window dimension. This is critical because if the AWBs are properly constructed, then the dominant basis function along the window axis should be around the DC component (representing little to no variation along the window axis in the simplified case that all windows have the same signal, a monodip event for example). Other than this modification, no other changes are required to be made for the original POCS iteration steps as describes in Abma et al., 2006.

An important part of a regular POCS iteration is the selection of an initial threshold and then subsequently lowering it with iterations such that more and more significant components of the signal are allowed to enter the solution. However for BAPOCS an important distinction from regular POCS is that the sparsity is enforced on a window-block and not individual windows. This makes the choice of the threshold more complicated (Li, 2008) both for computation speed as well as quality. Following Li, 2008, we use a soft thresholding scheme where the local variance of the window block is chosen as the soft thresholding parameter. Intuitively this makes sense as the local variance of the block is an estimate of the interpolation noise within the block that we are trying to remove. Also to handle potential blurring effects in the reconstruction due to the involvement of multiple windows within the block, the soft thresholding scheme is alternated with a Wiener Filtering towards the end of the iterative process (the final 10-15% iterations).

Once the final POCS iteration of the AWB is complete, we obtain a regularized estimate of all the windows that make up that block. We make a simplifying choice here and only update the primary window of interest (red window in Figure 1) as the final solution. However other reconstructed windows within the block are maintained in a buffer to aid in the construction of AWBs for the next primary window of interest.

Figure 2b shows a comparison of the uplift obtained using BAPOCS when compared to a regular POCS, 2a, for a real shot gather from a WAZ survey (far cable zoom shown) in which 85% traces were randomly removed (blue inset box in 2a) and reconstruction was attempted. Notice the improved continuity of events within the black circles and arrows in 2(b) compared to 2(a) as well as the reduction in the regularization noise indicated by the green circle and the arrows. Notice that for the input decimated data (blue inset box), computation of similar windows would be difficult and corrupted due to the large number of missing

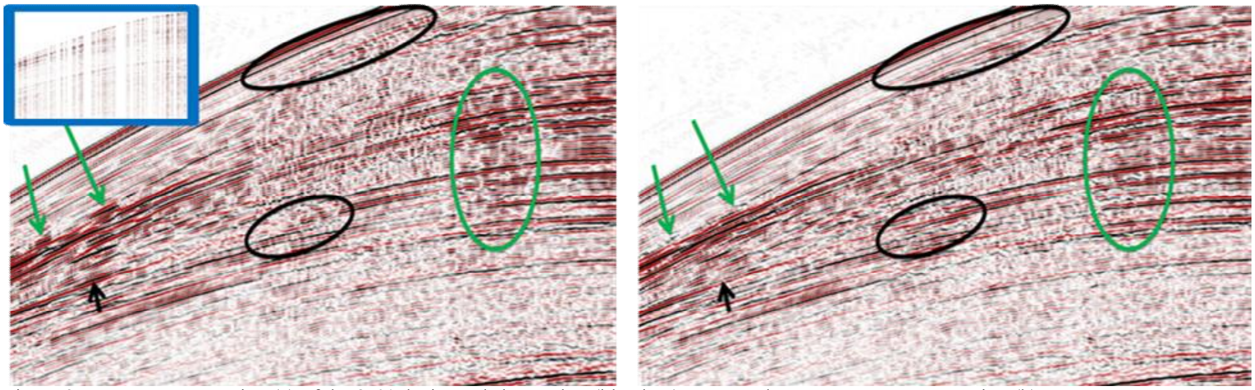

Figure 2. POCS reconstruction (a) of the 85% decimated shot gather (blue box) compared to BAPOCS reconstruction (b).

traces. In such a case a simple strategy is to run a 20 Hz low frequency reconstruction of the gathers with regular POCS, construct AWBs as per Step 1 on this initial estimate and then begin the step 2 BAPOCS iteration.

Application to RTM imaging

We show the uplift of using BAPOCS on field data by first attempting regularization of a shallow water NAZ dataset. Figure 3(a) shows the RTM inline image using the conventional partial NMO (PNMO) based RTM regularization. Notice the improved continuity of shallow sediments in the BAPOCS RTM image (3b) in the red box and red arrow, sharpening of a steep major fault plane (yellow arrow) and sharpening of smaller faults bunched together (yellow boxes). In general the swing noise is also reduced significantly throughout the section when compared to Figure 3a.

Figure 4a shows an oblique line, also in the sediment area, for a WAZ dataset from GOM. Again notice the significant improvement in event continuity, noise reduction, increased fault plane fidelity for the BAPOCS RTM image (4b) when compared to 4a. The depth slices for BAPOCS (Figure 4d) through the major faults in the area clearly indicate the increase in sharpness as well as reduction in swing noise compared to 4c. For this same dataset we now concentrate on the subsalt events where a series of dipping events are observed (Figure 5a). The dipping structures show breaks and unclear imaging in the original RTM (Figure 5a) as indicated by the arrows. This breaks in the imaging are also clearly seen in the depth slice as well (Figure 5c, yellow box). On the other hand for BAPOCS, the events are imaged with improved continuity (Figure 5b) Both continuity and amplitude is maintained for the events Notice the depth slice for BAPOCS (5d) clearly shows this improved continuity that we obtain using our BAPOCS regularization scheme.

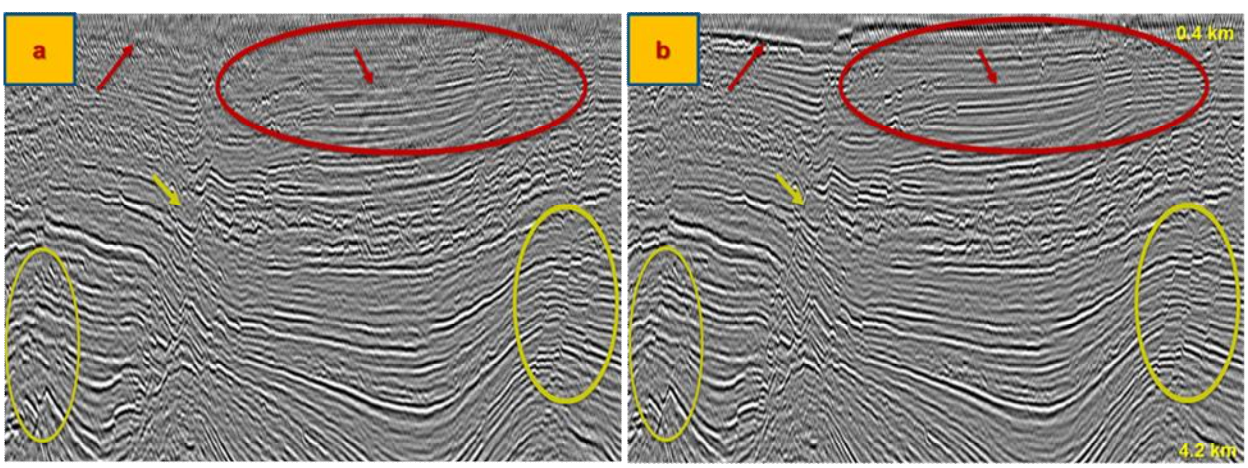

Figure 3. Stacked RTM image of a shallow water dataset using PNMO based regularization (a) and our method (b).

Conclusions

We have described a method that is able to introduce nonlocal processing techniques into the problem of seismic data regularization. We have shown that allowing local windows to communicate with each other using adaptive window blocks (AWB), allows signal reconstruction in a transform domain to be much easier by improving the sparsity as well the low-rank structure of the dataset. RTM imaging results for field data regularized with our BAPOCS method show the significant uplift that can be obtained. In general our method turns a *d*-dimensional regularization problem into *(d+1)*-dimensional problem by creating an added dimension referred to as the window-dimension. For computational efficiency the number of elements (contributing windows) in the added dimension is kept small (much smaller than a true 4D seismic regularization). Also unlike existing regularization schemes for supershots which tend to work on a shot-by-shot basis, our nonlocal schemes allows crosshot information to be included, increasing the robustness

Acknowledgements

We thank Zhiming Li, Jean Ji and Xinyi Sun for their helpful comments and discussions. We thank Connie VanSchuyver for help with the proof reading. We also thank TGS management for the permission to show the multiclient WAZ and NAZ datasets used in the paper

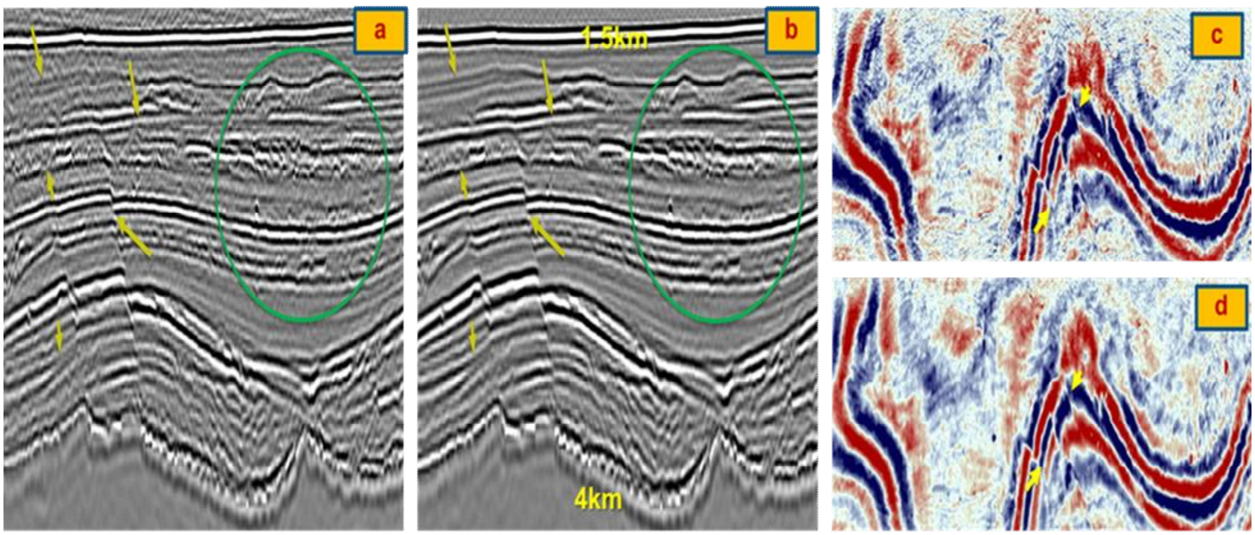

Figure 4. Stacked RTM image (Oblique line) of a WAZ dataset in sedimentary area using PNMO based regularization (a) and our method (b), corresponding depth slice at 3.5km (c) and (d).

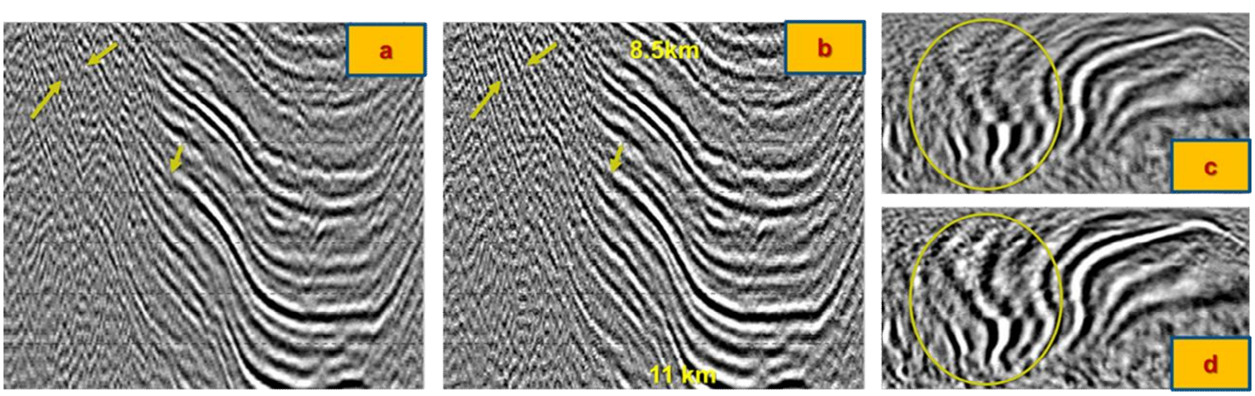

Figure 5. Subsalt dipping structures for WAZ Inline RTM image using PNMO regularization (a) and our method (b), corresponding depth slice at 9.5km (c) and (d).

EDITED REFERENCES

Note: This reference list is a copyedited version of the reference list submitted by the author. Reference lists for the 2017 SEG Technical Program Expanded Abstracts have been copyedited so that references provided with the online metadata for each paper will achieve a high degree of linking to cited sources that appear on the Web.

REFERENCES

Abma, R. and N. Kabir, 2006, 3D Interpolation of irregular data with a POCS algorithm: Geophysics, **71**, no.6, E91–E97, http://dx.doi.org/10.1190/1.2356088.

Buades, A., B. Coll, and J. M. Morel, 2005, A non-local algorithm for image denoising: Computer vision and pattern recognition, CVPR 2005, 2, 60–65.

Buades, A., B. Coll, and J. M. Morel, 2011, Self-similarity based image denoising: Communications of the ACM, 54, no. 5, 109–117, http://dx.doi.org/10.1145/1941487.1941513.

Dabov, K., A. Foi, V. Katkovnik, and K. Egiazarian, Image denoising by sparse 3D transform-domain collaborative filtering: IEEE Transactions Image processing, 16, no. 8, 2080-2095, http://dx.doi.org/10.1109/TIP.2007.901238.

Su, X. and T. Khoshgoftaar, 2009, A survey of Collaborative Filtering techniques: Advances in Artificial Intelligence, 2009, Article ID 42145, 19 pages, http://dx.doi.org/10.1155/2009/421425.

Wang, P. and K. Nimsaila, 2014, Fast progressive sparse Tau-p transform for regularization of spatially aliased seismic data: 84th Annual International Meeting, SEG, Expanded Abstracts, 3589–3593, https://doi.org/10.1190/segam2014-0889.1.

Xin, L., 2008, Patch-based image interpolation: algorithms and applications: International workshop on local and non-local approximation in image processing.

Xu, S., Y. Zhang, D. Pham, and G. Lambare, 2005, Antileakage Fourier transform for seismic data regularization: Geophysics, **70**, no.4, V87–V95, http://dx.doi.org/10.1190/1.1993713.